Landau-level mixing and spin degeneracy in the quantum Hall effect

V. Kagalovsky,* B. Horovitz, and Y. Avishai
Department of Physics, Ben-Gurion University of the Negev, Beer-Sheva, Israel
(Received 16 October 1996)

We study the dynamics of electrons in a magnetic field using a network model with two channels per link with random mixing in a random intrachannel potential; the channels represent either two Landau levels or two spin states. We consider channel mixing as a function of the energy separation of the two extended states and show that its effect changes from repulsion to attraction as the energy separation increases. For two Landau levels this leads to level floating at low magnetic fields, while for Zeeman-split spin states we predict level attraction at high magnetic fields, accounting for electron spin resonance data. We also study random mixing of two degenerate channels, while the intrachannel potential is periodic (nonrandom). We find a single extended state with a localization exponent $\nu \approx 1.1$ for real scattering at nodes; the general case also has a single extended state, though the localized nature of nearby states sets in at unusually large scales. [S0163-1829(97)02611-8]

I. INTRODUCTION

The quantum Hall effect (QHE) remains a great attraction for theoreticians and experimentalists. Of particular interest is the divergence of the localization length at a discrete set of energies, corresponding to extended states. This has motivated a large variety of methods for studying the pertinent metal-insulator transition as a critical second-order phase transition,[1] such as field-theoretical methods,[2] semiclassical methods,[3,4] numerical methods,[5] and finite-size scaling for transfer matrices.[6] Most of these works focus on properties near an isolated extended state with emphasis on the critical exponent ν of the localization length. The most recent experimental result[7] $\nu = 2.3 \pm 0.1$ is in agreement with theoretical predictions.[4,6]

The situation with a few extended states, allowing for coupling between these states, received less attention. This situation is relevant to the behavior of delocalized states in weak magnetic fields. It is well known that the existence of delocalized states is a necessary condition for the QHE behavior. On the other hand, scaling theory[8] and numerical studies[9] imply that in a two-dimensional (2D) system in the absence of a magnetic field all states should be localized. Therefore, a scenario in which delocalized states ''float up'' above the Fermi level as the magnetic field decreases has been suggested.[10,11] Recent experiments[12] show that, indeed, the energy of the lowest delocalized state floats up above the Fermi level as the magnetic field is reduced. This corresponds to a transition from an insulator to a quantum Hall conductor at both low and high fields. Numerical studies of a few Landau bands[13–17] focused on critical exponents, except for an early work by Ando,[5] which supports the floating scenario. Ando's work used δ-function impurities, which is, however, not suitable when the impurity concentration is too low since bound states of the δ potential shift the extended state even for a single Landau band.[5] We have recently shown[18] that two extended states attract each other, which leads to a minimum in the energy of the lower state. This attraction has also been predicted theoretically by Shahbazyan and Raikh[19] using a high-magnetic-field expansion.

The system of two coupled extended states was also studied in the context of a spin-split Landau band.[13–17] In the absence of a Zeeman term it was found that two separate extended states appear, each with a localization exponent of ≈ 2.3. Allowing for a finite Zeeman term leads to level attraction at high fields.[18] In fact, electron spin resonance (ESR) data[20] have shown that the spin splitting has an unusual nonlinear dependence on field. As shown below, this nonlinear dependence is consistent with localization phenomena and level attraction of extended states.

A different type of system where two degenerate states in a strong field (e.g., spin states in the first Landau level) are coupled by random mixing, but the scalar (i.e., intrachannel) potential is absent, was recently studied.[16,17,21,22] This corresponds to a spin-orbit coupling that is dominant relative to the scalar potential scattering. For white-noise interband mixing[21] it was found that an extended state at the original Landau-level energy exists, suggesting a distinct universality class. For smooth interband disorder,[22] it was suggested that there are two separate extended states as in the spin-split case in addition to a third extended state in between, at the original Landau level.

In the present work we study these and other aspects, using various extensions of the network model introduced by Chalker and Coddington.[6] In the network model electrons move along unidirectional links that form a closed loop in analogy with semiclassical motion on contours of constant potential. Scattering between links is allowed at nodes, in analogy with tunneling through saddle-point potentials in the semiclassical model. The assumption that each link carries current only in one direction implies that the wave packets are sufficiently localized in the transverse direction, i.e., the magnetic length is small in comparison to the spacing of nodes or with the correlation length of the potential fluctuations.

Our paper is organized as follows. In Sec. II we describe

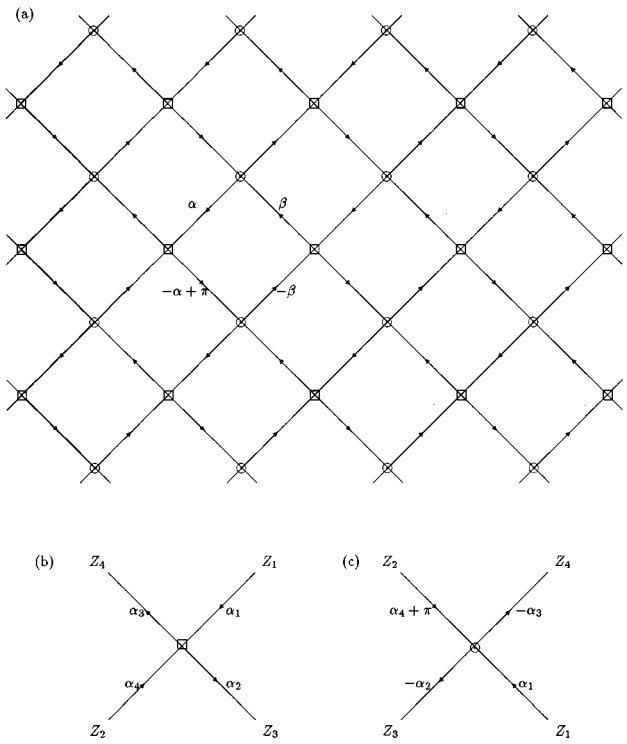

FIG. 1. Network model. Arrows indicate the direction of current flow. The nodes marked by ○ and □ are related by a 90° rotation. (a) The strip has M_l links with periodic boundary conditions ($M_l=6$ in the figure). In the two-channel case each link represents two channels, i.e., $M=2M_l$ is the number of transverse channels. The thick line is a reference for measuring area in Sec. IV. (b) and (c) Phase relations for two neighbor nodes.

the network model for one and two channels and relate parameters of the system to the transfer matrix. In Sec. III we expand our earlier work[18] and study the two-channel network model corresponding to two coupled Landau bands. We evaluate the energies of extended states as function of Δ, the bare energy separation of extended states in the absence of level mixing. In Sec. IV we investigate the two-level system with random mixing while the scalar potential scattering is periodic (i.e., nonrandom) and consider different types of symmetries for random mixing. Our results are summarized in Sec. V, where the ESR data are also discussed. In Appendix A, using the one-channel network model, we test the possibility of sublocalization behavior of the wave function, based on a possible fractal behavior of the nodes. In Appendix B the tunneling amplitude between Landau levels is estimated.

II. THE NETWORK MODEL

Consider first a one-channel Chalker-Coddington (CC) network,[6] which has directed links and scattering at nodes [Fig. 1(a)]. Propagation along links yields a random phase ϕ, thus links are presented by diagonal matrices with diagonal elements in the form $\exp(i\phi)$. The transfer matrix for one node relates a pair of incoming and outgoing links on the left [links 2 and 4 in Fig. 1(b)] to a pair of links on the right (links 1 and 3); it has the form

$$\mathbf{T}=\begin{pmatrix} e^{i\alpha_1} & 0 \\ 0 & e^{i\alpha_2} \end{pmatrix} \begin{pmatrix} \cosh\theta & \sinh\theta \\ \sinh\theta & \cosh\theta \end{pmatrix} \begin{pmatrix} e^{i\alpha_3} & 0 \\ 0 & e^{i\alpha_4} \end{pmatrix}. \tag{1}$$

In order for the system to be invariant, on average, under 90° rotation the next-neighbor node is obtained by rotating Fig. 1(b) by 90° and writing the states on links 4 and 1 in terms of those on links 2 and 3. The transfer matrix then has the same form as in Eq. (1) with a parameter θ' replacing θ, where[6] $\sinh\theta'=1/\sinh\theta$ and the phases $\alpha_1,\alpha_2,\alpha_3,\alpha_4$ are replaced by $-\alpha_3,\alpha_1,\alpha_4+\pi,-\alpha_2$ [Fig. 1(c)]. We therefore describe scattering at the nodes indicated in Fig. 1 by circles with transfer matrix $\mathbf{T}(\theta)$ and at the nodes indicated by boxes with $\mathbf{T}(\theta')$.

The phases α_i can be absorbed into phases describing propagation on links. Since a shift by a common phase in all links of a given column does not affect the Lyapunov exponents of the network, we can choose the phases on the links as $\pm\alpha,\pm\beta$ [Fig. 1(a)], where $\alpha=\frac{1}{2}\alpha_1-\frac{1}{2}\alpha_4-\alpha_2$ and $\beta=\frac{1}{2}\alpha_1-\frac{1}{2}\alpha_4+\alpha_3$. Note that the sum of left links equals those of right links $+\pi$. For a random potential (Sec. III) these link phases are considered as random, while for a periodic potential (Sec. IV) we choose specific sets. The appropriate procedure is then to multiply transfer matrices for links and nodes alternately and derive Lyapunov exponents for strips of width up to 64 and of length of typically 60 000 units (Sec. III) or 240 000 (Sec. IV). At these lengths our error for the localization length (i.e., for the inverse of the smallest Lyapunov exponent) is $\lesssim 0.5\%$.

In the following we relate the node parameter θ to the electron energy by using known results for scattering from a saddle-point potential.[23] The transmission probability T of an electron with energy E through a saddle-point potential $V_{\mathrm{SP}}(x,y)=-U_x x^2+U_y y^2+V_0$ in a perpendicular magnetic field B is given by

$$T=\frac{1}{1+\exp(-\pi\epsilon)}, \tag{2}$$

where

$$\epsilon\equiv[E-(n+\tfrac{1}{2})E_2-V_0]/E_1, \tag{3}$$

and

$$E_1=\left[\Omega\left\{\gamma^2+\left(\frac{\omega_c}{4}\right)^2\right\}^{1/2}-\frac{1}{4}\Omega^2-\left(\frac{\omega_c}{4}\right)^2\right]^{1/2}, \tag{4}$$

where $\Omega=[\frac{1}{4}\omega_c^2+(U_y-U_x)/m]^{1/2}$, $\gamma=(U_y+U_x)/4m\Omega$, m is the electron mass, and $\omega_c=eB/mc$ is the cyclotron frequency. The oscillator frequency E_2 is

$$E_2=2\left[\Omega\left\{\gamma^2+\left(\frac{\omega_c}{4}\right)^2\right\}^{1/2}+\frac{1}{4}\Omega^2+\left(\frac{\omega_c}{4}\right)^2\right]^{1/2}. \tag{5}$$

From Eq. (2) the ratio of reflection and transmission coefficients is $\exp(-\pi\epsilon)$. On the other hand, the transfer matrix Eq. (1) determines this ratio as $(\sinh\theta)^2$. Therefore, the relation between node parameter θ in the CC model and the electron energy is

$$\epsilon = -\frac{2}{\pi}\ln(\sinh\theta). \tag{6}$$

We note that unlike discrete Landau levels, the saddle-point potential allows for a continuous energy E for each discrete state n. Furthermore, for $\omega_c \gg \gamma$, $E_1 \to 0$, $E_2 \to \omega_c$, and $E \to \hbar\omega_c(n+1/2)+V_0$ corresponds to discrete Landau levels. In the opposite limit of $\omega_c \ll \gamma$ we have $E_1 \to (U_x/2m)^{1/2}$, $E_2 \to (2U_y/m)^{1/2}$, and the integer n corresponds to a quantum number of the harmonic potential $U_y y^2$.

In the case of one channel per link a single extended state[6] is at $\epsilon = 0$ (i.e., $\theta = 0.8814$), corresponding to the center of any band n, $E = (n+1/2)E_2 + V_0$. Numerical studies of this system with width M and periodic boundary conditions confirm the one-parameter scaling hypothesis, i.e., the localization length ξ_M is given by a scaling function f, where

$$\frac{\xi_M}{M} = f\left(\frac{M}{\xi(E)}\right), \tag{7}$$

with $\xi(E) \sim |E|^{-\nu}$ and $\nu = 2.5 \pm 0.5$. This result is in good agreement with experimental data for spin resolved levels,[7] numerical simulations using other models,[16,24] and a semiclassical derivation[4,25] that predicts $\nu = 7/3$. We have repeated the one-channel calculation (Appendix A) with particular emphasis on the possibility of sublocalization; we find that localized states decay as a regular exponential.

A two-channel network, i.e., two channels per link, is characterized by parameters θ and $\theta - \Delta\theta$, which determine the tunneling amplitude at the node for each channel with $\Delta\theta$ related to the relative energy interval between the bands of the two channels. The transfer matrix is parametrized as[14]

$$\mathbf{T} = \begin{pmatrix} \mathbf{U}_1 & 0 \\ 0 & \mathbf{U}_2 \end{pmatrix} \begin{pmatrix} \mathbf{C} & \mathbf{S} \\ \mathbf{S} & \mathbf{C} \end{pmatrix} \begin{pmatrix} \mathbf{U}_3 & 0 \\ 0 & \mathbf{U}_4 \end{pmatrix}. \tag{8}$$

The transfer matrix at a node is composed of the blocks

$$\mathbf{C} = \begin{pmatrix} \cosh\theta & 0 \\ 0 & \cosh(\theta - \Delta\theta) \end{pmatrix}, \quad \mathbf{S} = \begin{pmatrix} \sinh\theta & 0 \\ 0 & \sinh(\theta - \Delta\theta) \end{pmatrix}. \tag{9}$$

Defining an energy parameter Δ such that $\epsilon - \Delta = -(2/\pi)\ln(\sinh(\theta - \Delta\theta))$, we obtain

$$\mathbf{C} = \begin{pmatrix} \sqrt{1+\exp[-\pi(\epsilon-\Delta)]} & 0 \\ 0 & \sqrt{1+\exp[-\pi\epsilon]} \end{pmatrix},$$

$$\mathbf{S} = \begin{pmatrix} \exp[-\pi(\epsilon-\Delta)/2] & 0 \\ 0 & \exp[-\pi\epsilon/2] \end{pmatrix}. \tag{10}$$

Propagation along links yields random phases $\phi_i, i = 1-4$, and also allows mixing between two different channels. It is described by block $\mathbf{U}$:

$$\mathbf{U} = \begin{pmatrix} e^{i\phi_1} & 0 \\ 0 & e^{i\phi_2} \end{pmatrix} \begin{pmatrix} \sqrt{1-x^2} & -x \\ x & \sqrt{1-x^2} \end{pmatrix} \begin{pmatrix} e^{i\phi_3} & 0 \\ 0 & e^{i\phi_4} \end{pmatrix}, \tag{11}$$

where x^2 is the mixing probability between different levels.

We note that the maximal number of independent parameters in a U(2) matrix presented in Eq. (11) is 4. These phases can be chosen as $\delta = 1/2(\phi_1+\phi_2+\phi_3+\phi_4)$, $\delta_1 = -1/2(\phi_2+\phi_4)$, and $\delta_2 = -1/2(\phi_2-\phi_3)$ so that

$$\mathbf{U} = e^{i\delta}\begin{pmatrix} e^{i\delta_1}\sqrt{1-x^2} & -e^{i\delta_2}x \\ e^{-i\delta_2}x & e^{-i\delta_1}\sqrt{1-x^2} \end{pmatrix}. \tag{12}$$

The phase δ corresponds to a scalar potential; it can be either random (Sec. III) or fixed for a periodic potential (Sec. IV). If $\delta = 2\pi\mathcal{I}$ (where $\mathcal{I}$ denotes an integer), the $\mathbf{U}$ matrix changes its symmetry group from U(2) to a unitary unimodular SU(2). In Sec. IV we study the effect of various subgroups of U(2) on the critical properties of the system.

III. NONDEGENERATE LEVELS WITH RANDOM POTENTIAL AND RANDOM MIXING

We study here a system of two Landau levels in the presence of a smooth random potential, so that for proper description we use the most general form of Eq. (12) with four random variables. In the absence of level mixing we know from results of the one channel system[6] that $\epsilon = 0$ corresponds to extended states. This defines ''bare'' extended states at $E_{\rm ex} = E_2(n+1/2)+V_0$ and the bare energy splitting of the $n = 0,1$ states is then E_2. Note that the splitting E_2, which is magnetic-field dominated at $\omega_c(m/U)^{1/2} > 1$, remains finite as $\omega_c \to 0$ and is potential dominated at $\omega_c(m/U)^{1/2} < 1$ (here $U_x = U_y \equiv U$). The latter region is acceptable for a network model if the correlation length of the potential fluctuation is long compared to the magnetic length, so that locally the saddle-point potential determines a finite splitting. The splitting $\Delta = E_2/E_1$ is therefore bounded by $\Delta \geqslant 2$ at $\omega_c \to 0$.

The application to $n = 0,1$ Landau levels assumes that mixing of states with n's differing by $\Delta n = 2$ is much smaller than for those with $\Delta n = 1$. Mixing or transition rates can be evaluated for a potential of the form $(1/2)\tilde{U}(x^2+y^2) - \tilde{U}y^3/\lambda$, where λ is a measure of the correlation length of the random potential. For states near the local minimum we find that mixing is given by Eq. (B6) (see Appendix B). We therefore expect our results for the $n = 0$ state, within the two channel model, to be valid down to $m\omega_c^2/U \approx 1/\ln(\lambda/l) \lesssim 1$ (assuming $\tilde{U} \approx U$) so that the range of valid $m\omega_c^2/U$ values is extended down to lower limits for longer-range potential fluctuations. The results for the $n = 1$ state, however, are not directly relevant.

We consider below also the case of a spin-split single level $n = 0$ for which $V_0 = \pm(1/2)g^*\mu_B$, where g^* is the electron g factor and μ_B is the Bohr magneton. The bare extended states then correspond to $E_{\rm ex} = \frac{1}{2}E_2 \pm \frac{1}{2}g^*\mu_B$, so that $\Delta = g^*\mu_B/E_1$.

The system [see Eqs. (8) and (10)] is, on average, invariant under 90° rotation if at the next-neighbor node the transmission and reflection (of each channel) are interchanged,

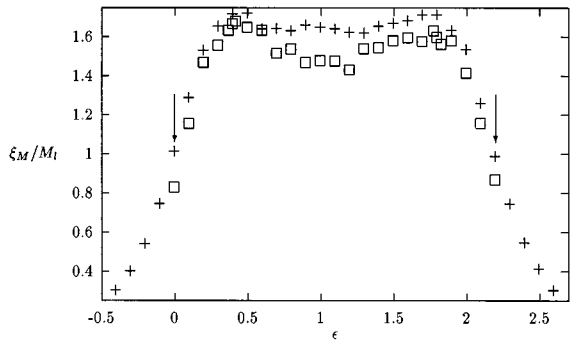

FIG. 2. Renormalized localization length ξ_M/M as a function of ϵ for $\Delta=2.2$. +'s correspond to $M=32$ and □'s to $M=64$ system widths. Arrows point to the location of extended states in the absence of level mixing. The energies of extended states (near the peaks of ξ_M/M_l) are closer than the arrow positions, demonstrating level attraction.

i.e., $\epsilon\rightarrow-\epsilon$ and $\epsilon-\Delta\rightarrow-\epsilon+\Delta$. The system is then symmetric under $\epsilon\rightarrow-\epsilon$, $\Delta\rightarrow-\Delta$ and the extended states at ϵ_i $(i=1,2)$ become $\epsilon_i(-\Delta)=-\epsilon_i(\Delta)$. A further translation of energies by Δ returns the system to itself except for a $1\leftrightarrow2$ interchange; $\epsilon_2(-\Delta)+\Delta=\epsilon_1(\Delta)$, hence $\epsilon_1(\Delta)+\epsilon_2(\Delta)=\Delta$. Therefore, results for the two energies $\epsilon_{1,2}$ are constrained by the condition $\epsilon_1+\epsilon_2=\Delta$.

We proceed further by calculating normalized localization length ξ_M/M_l for systems with $M=16,32$ (the size of the **T** matrix is $M\times M$ and $M_l=M/2$ is the number of links across the strip) and different values of ϵ and Δ. For $\Delta=0$ we used also $M=64$, which affected critical energies by 3%, which is within 5% from the result of Wang *et al.*[15] The coupling x is chosen to be uniformly distributed in the interval $[0,1]$; we checked that other distributions in x lead to similar results. Finite-size scaling is then used for fitting our data onto a single curve $f(\xi_\infty(\epsilon)/M_l)$ extracting values of localization length ξ_∞ for the infinite 2D system. Finally, we look for the critical energies ϵ_i and critical exponent ν by requiring $\xi_\infty\sim|\epsilon-\epsilon_i|^{-\nu}$. The raw data for one particular Δ (see Fig. 2) represents the characteristic features of the system. One can see that the values of ξ_M/M_l for any two energy values whose sum equals Δ coincide, as we expect from the symmetry condition. Another important feature is that for $\Delta\gtrsim1$ we have two pronounced maxima of ξ_M/M_l, which we expect to be near the critical energies; this is supported by the scaling procedure. We find that approaching the critical energies from outside yields $\nu=2.5\pm0.5$. The states between the two critical energies seem to be localized, i.e., ξ_M/M_l decreases with M, although the decrease is rather slow.

The critical values $\epsilon_{1,2}$ are presented as a function of Δ in Fig. 3. We cannot calculate ξ_M/M for $\Delta>3.5$ because of roundoff errors. The $\Delta\rightarrow\infty$ case can be solved analytically,[19] since then, near one extended state the other channel is very far from tunneling and its trajectory is a closed loop between the nodes. Eliminating the closed loop variables and assuming that it mixes with links of only one node leads to extended states at $\epsilon_1(\Delta)\sim1/\Delta$ and $\epsilon_2(\Delta)-\Delta\sim-1/\Delta$. The rather flat behavior of $\epsilon_1(\Delta)$ up to $\Delta<3.5$ implies that the asymptotic behavior[19] sets in at a higher Δ.

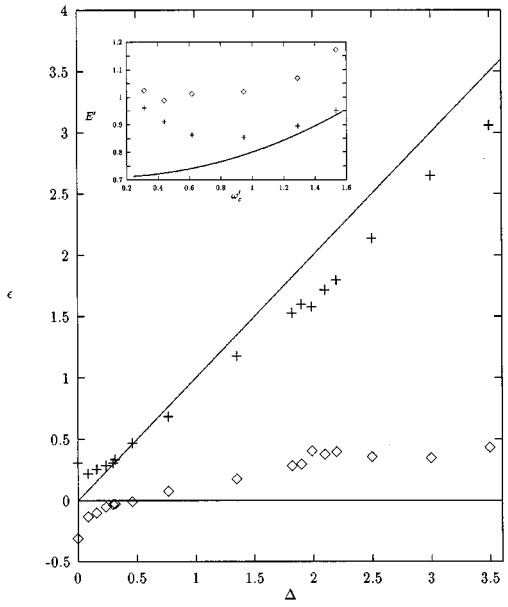

FIG. 3. Critical values ϵ as functions of Δ. Full lines are the bare extended states $\epsilon=0$ and $\epsilon=\Delta$ are shown. Inset: energy of the lowest extended state as a function of magnetic field with full level mixing (◇) and with reduced mixing (+). The full line is the lowest bare extended state. Here $E'=E(2m/U)^{1/2}$ and $\omega_c'=\omega_c(2m/U)^{1/2}$.

The most remarkable aspect of the data is the crossing of $\epsilon_i(\Delta)$ with the bare extended states at $\Delta\approx0.5$. Usually one expects that mixing affects mainly extended states leading to level repulsion of these states. This expectation leads to $\epsilon_1(\Delta)$ approaching zero from below and $\epsilon_2(\Delta)$ approaching Δ from above, as implied by Fig. 2 of Ref. 13. Contrary to this expectation we find that above $\Delta\approx0.5$ there is level attraction.

Level attraction is also supported by the following observation: Parametrize the upper branch of critical ϵ by θ, i.e., $\epsilon=-(2/\pi)\ln\sinh\theta$; at $\Delta=0$, $\epsilon=0.23$, i.e., $\theta=0.65$,[13,15] and ϵ increases with Δ so that $\theta\rightarrow0$. In the level repulsion scenario $\epsilon>\Delta$ so that the parameter $\Delta\theta$ in Eq. (9) varies in the range $0\geqslant\Delta\theta\geqslant-0.88$. We could, however, define the model with parameters $\theta,\Delta\theta$ (instead of ϵ,Δ) with $\Delta\theta$ unbounded, which implies that $\epsilon-\Delta$ must change sign.

We present now results for the energies of extended states as a function of magnetic field by relating Δ to B via Eqs. (5) and (6). As noted above E_2 is always finite so that $\Delta\geqslant2$ ($\Delta\rightarrow2$ for $B\rightarrow0$ and $U_x=U_y$) and thus we are always in the level attraction regime. The results are shown in the inset of Fig. 3 by diamonds (assuming, for simplicity, $U_x=U_y\equiv U$) and the full line is the lower bare extended state energy. Our data show a minimum at $\omega_c(2m/U)^{1/2}\approx0.5$ in the lower state, consistent with floating, and are a result of level attraction due to Landau-level mixing. Allowing for mixing with the $n=2$ Landau level may cause floating of the $n=1$ state as well, but will have a small effect on the floating of the $n=0$ state, as discussed above. For N Landau levels our symmetry argument shows that the extended state energies come in pairs whose average is the same as for the bare states, i.e., $\epsilon_i+\epsilon_{N+1-i}=(N-1)\Delta$, with $i=1,\ldots,N$. Hence

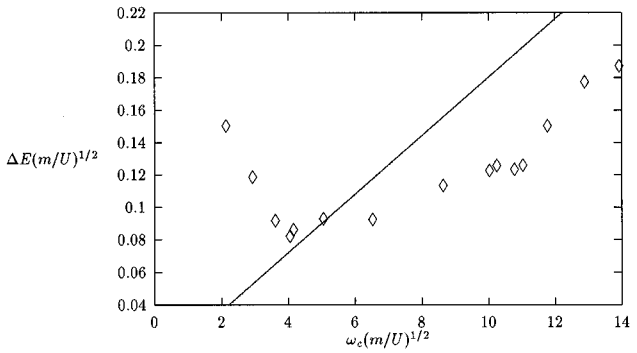

FIG. 4. Energy of spin splitting of extended states ($\diamond$'s) with bare splitting (straight line) of $g^*\mu_B B = 0.018\omega_c$. GaAs/$Al_xGa_{1-x}$As data (Ref. 20) fit our results with $(U/m)^{1/2} = 310$ GHz and the field scale is $\omega_c(U/m)^{1/2} \approx 1.3B$ T.

we expect that the energies of the lower half states increase at low fields, consistent with the floating scenario and with the experimental data.[12]

The assumption of full mixing, i.e., $x \in [0,1]$ in Eq. (11), is not valid for strong magnetic fields where tunneling between Landau levels should be suppressed. We model this situation in a reduced mixing model (see Appendix B), where the parameter x in Eq. (12) is now chosen randomly in the reduced range of $[0,\exp(-m\omega_c^2/U)]$. The results are shown in the inset of Fig. 3 by pluses. The minimum in the lower level is now more pronounced and is at a higher field the $\omega_c(2m/U)^{1/2} \approx 1$.

Finally, we present the application of our data to extended state energies for a Zeeman spin splitting of a Landau band where $\Delta = g^*\mu_B B/E_1$. Since Δ can cross the value ≈ 0.5 we predict that spin splitting is larger than expected for small fields (level repulsion) and is smaller than expected for large fields (level attraction). In fact, we claim that level attraction accounts for ESR data,[20] which show a nonlinear dependence of the spin splitting on B. In particular, the data for $N=0$ in the range $8-14$ T is visibly nonlinear in the range $8-12$ T.

To demonstrate the effect we consider $g^*\mu_B B/\omega_c = g^* m/2m_0 = 0.018$ (e.g., $g^* = 0.51$ with an effective to free electron mass ratio of[28] $m/m_0 = 0.07$) and replot the data of Fig. 3 for the splitting $\Delta E = E_1(\epsilon_2 - \epsilon_1)$ in Fig. 4. The experimental data at $B > 8$ T fit our results if $(U/m)^{1/2} = 310$ GHz is chosen (see Sec. V for independent data leading to this value); the field scale is then $\omega_c(U/m)^{1/2} \approx 1.3B$ T. The deviation from a straight line measured at $8-12$ T cannot be accounted for by band-structure calculations (see Sec. V). The data, therefore, provide strong support for level attraction at these fields.

IV. DEGENERATE LEVELS WITH RANDOM MIXING

We consider in this section a single Landau level with two degenerate spin states (i.e., no Zeeman term) where the only randomness comes from mixing of the spin states, e.g., by spin-orbit scattering. A model of this type was studied by Hikami, Shirai, and Wegner[21] with the Hamiltonian

$$H = \frac{1}{2m}(\mathbf{p}+\mathbf{A})^2 + \mathbf{h}(\mathbf{r})\cdot\boldsymbol{\sigma}, \tag{13}$$

where $\mathbf{h}(\mathbf{r})$ is a random field in the x and y directions and projection to states of the lowest Landau level is understood. This model has an extended state at the original Landau level[21] ($\epsilon = 0$) and possibly two additional extended states,[22,16,17] symmetric around $\epsilon = 0$.

We wish to study the Hamiltonian [Eq. (13)] by a network model. We therefore replace the continuum by a periodic potential so that the nodes of the network are the periodic set of saddle points. In general, a magnetic flux through a unit cell leads to Aharonov-Bohm phases on the links that increase linearly from, say, left to right. This, however, reduces the symmetry around $\epsilon = 0$ as checked by our simulations; this may be related to the formal loss of invariance under 90° rotations. We therefore choose the unit cell to have an integer number of flux quanta.

As shown in Figs. 1(a) and 1(b), the phases on the links can be represented by two phases α, β. In order to choose relevant values of α, β we consider the pure system without spin mixing and try to make its spectra similar to that of the $\mathbf{p}^2/2m$ term in Eq. (13), i.e., a constant, with a total number of states close to that of a Landau level. Extended states in the pure system can be found by applying transfer matrices across a unit cell (i.e., two nearby nodes in Fig. 1), which by Bloch's theorem lead to multiplication by $\exp(iq)$ along the strip or $\exp(ik)$ in the direction across the strip. This procedure yields the dispersion relation

$$\cosh(\pi\epsilon/2) = \frac{\sin q + \sin(k-\alpha+\beta)}{2\sin(\alpha+\beta)}. \tag{14}$$

This relation shows that there is a maximal energy $\epsilon_{\max}$ in the band where $\cosh(\pi\epsilon/2) = 1/\sin(\alpha+\beta)$. The density of states is linear at $\epsilon \to 0$ and saturates at $\epsilon_{\max}$. The total number of states in the band approaches that of a Landau level for $\alpha+\beta \to 0$. However, at $\alpha+\beta = 0$ the spectra Eq. (14) is singular, so that it seems that a small but finite value of $\alpha+\beta$ is needed.

The spin term in Eq. (13) is taken to mix spin states on links. Since all links are unidirectional the transfer matrix is equivalent to an evolution operator that is a rotation in spin space $\exp[(i/\hbar)\int \mathbf{h}(\mathbf{r})\cdot\boldsymbol{\sigma}\, dt]$. Since successive rotations about the x and y axes produce a rotation about the z axis $\mathbf{h}$ should be a 3D vector. The effect of these rotations is equivalent to an SU(2) transfer matrix [Eq. (12) with $\delta = 0$] and we can interpret all independent phases as corresponding angles of the pseudofield. Below we consider such transfer matrices with different sets of independent parameters for the case of two degenerate levels.

Consider first the case when $\mathbf{T}$ is a real matrix, i.e., the pseudofield is only in the y direction and $\mathbf{T}$ then has SO(2) symmetry,

$$\mathbf{U} = \begin{pmatrix} \cos\phi & -\sin\phi \\ \sin\phi & \cos\phi \end{pmatrix}. \tag{15}$$

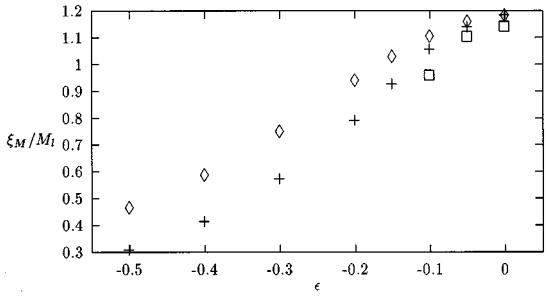

FIG. 5. Renormalized localization length ξ_M/M_l as a function of energy ϵ for a system with SO(2) mixing between the levels. $\diamond$'s correspond to $M=16$, $+$'s to $M=32$, and $\square$'s to $M=64$ system widths.

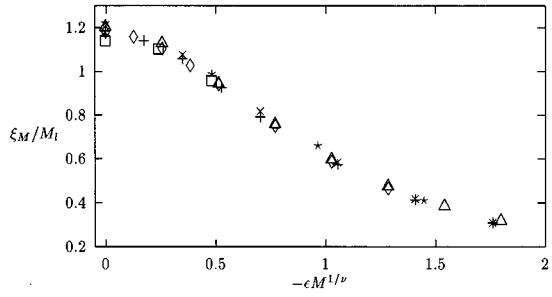

FIG. 6. Fit of raw data from Fig. 5 for a system with SO(2) and for a system with U(1)×SO(2) mixing between the levels: ξ_M/M_l versus $\epsilon M_l^{1/\nu}$ with $\nu=2.2$. $\diamond$'s correspond to $M=16$, $+$'s to $M=32$, and $\square$'s to $M=64$ system widths for SO(2) case; $\times$'s correspond to $M=16$, $\triangle$'s to $M=32$, and $\star$'s to $M=64$ system widths for the U(1)× SO(2) case.

The results for the case with the Haar measure, i.e., $\phi \in [0,2\pi]$ with $\cos\phi$ uniformly distributed, are shown in Fig. 5. The data show a single extended state at $\epsilon=0$.

We know that random U(2) transfer matrices lead to two extended states. It is therefore interesting to modify the SO(2) system by a random potential leading to a U(1)× SO(2) system

$$\mathbf{U}=e^{i\delta}\begin{pmatrix}\cos\phi & -\sin\phi\\ \sin\phi & \cos\phi\end{pmatrix}. \tag{16}$$

The data maintain a single peak at $\epsilon=0$ in this case as well. Fitting the data of those two cases by a smooth function f so that $\xi_M/M_l=f(\epsilon M_l^{1/\nu})$ yields $\nu\approx 2.2$ for the critical exponent (Fig. 6). Actually, one should expect in those two cases behavior similar to the one-channel model due to the fact that matrices **U** commute with each other. Our results support this expectation.

Next in the hierarchy of symmetries is the SU(2) group [Eq. (12) with $\delta=0$] with three independent phases. (A choice of two independent phases is not closed under successive transfer operations.)

The most general case of a network model corresponding to the Hamiltonian Eq. (13) is that of SU(2) matrices on links and a complex transfer matrix [Eq. (1)] at nodes. The **T** matrix on links is then a U(2) matrix; however, only its SU(2) phases are random, while the phase δ in Eq. (12) is regular, having the values $\pm\alpha,\pm\beta$ periodically.

Before presenting numerical results we discuss the symmetries for which $\xi_\infty(\epsilon)$ is invariant. Note first that $\alpha\to\alpha+\pi$ or $\beta\to\beta+\pi$ is a symmetry, since one can shift even or odd columns by a constant phase. Shifting by π results in $\alpha+\pi$ and $-\alpha+2\pi$ [the latter is equivalent to $-(\alpha+\pi)+\pi$] or $\beta+\pi$ and $-\beta+\pi$ (the latter is now equivalent to $-\beta-\pi$). Consider next the up-down reflection symmetry that yields (after shifts by π) the equivalence $(\alpha,\beta)\to(-\alpha,-\beta)$. The right-left reflection symmetry leads to $(\alpha,\beta)\to(\beta+\pi/2,\alpha-\pi/2)$. Indeed, looking from right to left, the links with phases $(\beta,-\beta)$ come first (actually with opposite signs since propagation is to the left, but by the previous symmetry signs can be changed), while $(\alpha,-\alpha+\pi)$ come second; shifting by $\pm\pi$, this yields the stated equivalence. The next symmetry is a property of the infinite 2D system: if we rotate our system by 90° and then shift the phases properly we get $(\alpha,\beta)\to((\alpha+\beta+\pi)/2,(\alpha+\beta-\pi)/2)$, but due to the right-left symmetry this is just $((\alpha+\beta)/2,(\alpha+\beta)/2)$. If this symmetry holds for our finite strips then it is sufficient to consider only the diagonals in the (α,β) plane. Note that all these symmetries hold for the spectra of the pure system Eq. (14). Finally, we consider a symmetry that is due to the random SU(2) phases. A shift of the link phase δ in Eq. (12) by π is equivalent to a shift of π in the SU(2) phases δ_1,δ_2; since the latter are random the result is invariant. Thus, in Fig. 1(a) the phase $-\alpha+\pi$ can be replaced by $-\alpha$ and a column shift by $\pi/2$ yields $(\alpha,\beta)\to(\alpha+\pi/2,\beta)$ or similarly $(\alpha,\beta)\to(\alpha,\beta+\pi/2)$. Thus, with rotation symmetry it is sufficient to consider phases (α,α) in the range $0<\alpha<\pi/4$.

We checked all these symmetries numerically. It turned out that all symmetries hold; however, the rotational symmetry requires larger M and a higher number of iterations than in the U(2) case, in particular for large α,β. This has the following probable explanation: the periodic phases α,β introduce a new irrelevant length scale in the system. In order to go beyond this scale to find the symmetries one needs to

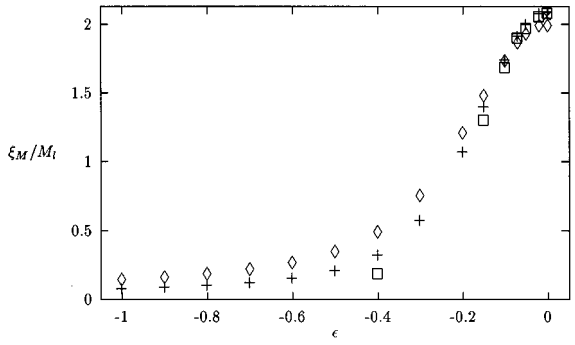

FIG. 7. Renormalized localization length ξ_M/M_l as a function of energy ϵ for a system with SU(2) matrices on links and and a complex transfer matrix at nodes with small $(\alpha=-0.175,\beta=0.075)$ phases after 480 000 iterations. $\diamond$'s correspond to $M=16$, $+$'s to $M=32$, $\square$'s to $M=64$, and $\times$'s to $M=128$ system widths.

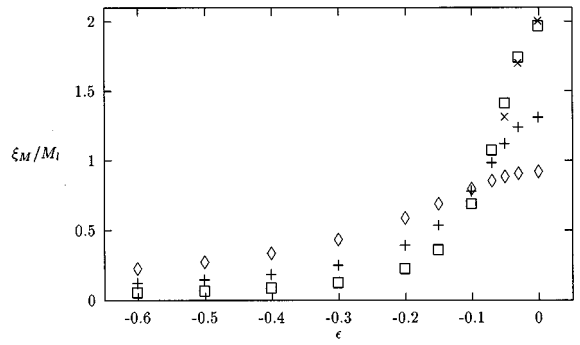

FIG. 8. Renormalized localization length ξ_M/M_l as a function of energy ϵ for a system with SU(2) matrices on links and a complex transfer matrix at nodes with small ($\alpha=\beta=-0.005$) phases after 480 000 iterations. $\diamond$'s correspond to $M=16$, $+$'s to $M=32$, $\square$'s to $M=64$, and $\times$'s to $M=128$ system widths.

investigate much longer systems [at least 300 000 iterations in comparison with 60 000 in the U(2) case]. The rotational symmetry was found for the largest system size $M=128$ for some particular phases. It is expected to hold for $M\to\infty$.

The results for $(\alpha=-0.175,\beta=0.075)$ and $(\alpha=-0.005,\beta=-0.005)$ are shown in Figs. 7 and 8 respectively. The data exhibit single peaks near $\epsilon=0$. The peculiar property of the data is that in the range between $\epsilon\approx-0.1$ and $\epsilon=0$ the renormalized localization length $\xi_{16}/8<\xi_{32}/16<\xi_{64}/32$, which indicates a band of extended states; however, the data for $M=128$ shows $\xi_{64}/32>\xi_{128}/64$, which determines these to be localized states. This is just another manifestation of the irrelevant length scale mentioned above.

We consider, finally, the case $\alpha=\beta=0$ in Figs. 9 and 10. Although the pure case is singular, the disordered system is well behaved, the data converge faster and there is no irrelevant length scale, i.e., the localized behavior of $\epsilon\neq0$ states sets in already at $M=32$. We therefore consider $\alpha=\beta=0$ as the generic case for SU(2).

There is clearly a single extended state at $\epsilon=0$ or, more precisely, at least all states with $|\epsilon|>0.03$ are localized. Recall, that in the U(2) case with $\Delta=0$ the extended states are, at $\epsilon\approx\pm0.2$, well separated from $\epsilon=0$ (see Refs. 13–15).

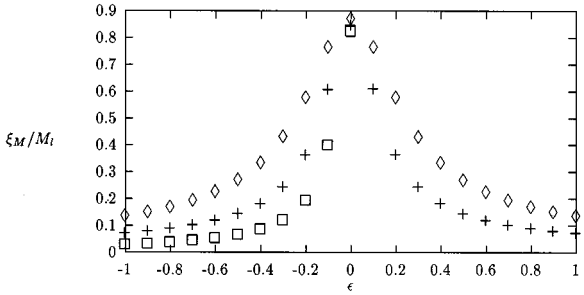

FIG. 9. Renormalized localization length ξ_M/M_l as a function of energy ϵ for a system with SU(2) mixing between the levels. $\diamond$'s correspond to $M=16$, $+$'s to $M=32$, and $\square$'s to $M=64$ system widths.

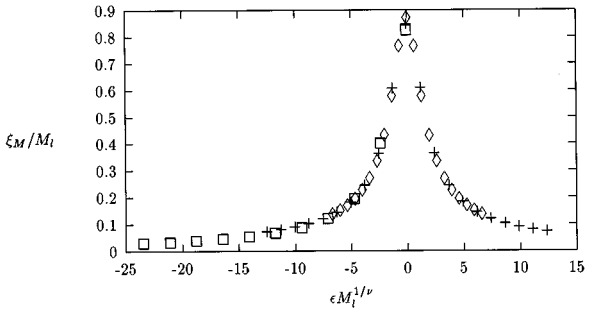

FIG. 10. Fit of raw data from Fig. 9 for a system with SU(2) mixing between the levels: ξ_M/M_l versus $\epsilon M_l^{1/\nu}$ with $\nu=1.1$.

Hence, if there are extended states in the SU(2) case near $\epsilon=0$, they are extremely close to $\epsilon=0$ and therefore are not related to those of the U(2) case as has been proposed.[22]

The critical exponent in Fig. 10 is $\nu\approx1.1$. Thus the SU(2) case is a distinct universality class. This is consistent with the occurrence of a singular density of states and the distinct value of σ_{xx} found by Hikami *et al.*[21]

Finally, we consider an interpolation between U(2) and SU(2) by allowing the link phase [δ in Eq. (12)] to be random in a restricted range of $p[-\pi,\pi]$. On long scales the randomness may accumulate, allowing an SU(2) behavior only at $p=0$. However, it is known that a metal-insulator transition (in the absence of a magnetic field) occurs at a finite ratio of spin-orbit to scalar randomness.[26] Thus it may be possible that SU(2) behavior sets in at a finite p. Figure 11 shows our data with $p=0.3$; the best fit for the scaling form yields extended states at $\epsilon=\pm0.16$ with $\nu=2.5$. Since the extended states of the U(2) case ($p=1$) are at $\epsilon\approx\pm0.2$,[13–15] we conclude that the two extended states approach each other as p is reduced, until below $p\approx0.2$ they merge and only $\epsilon=0$ corresponds to an extended state (or states). The range between $p\approx0.2$ and $p\approx0.05$ is difficult to analyze since the localized nature of the states near $\epsilon=0$ sets in only at $M=128$; apparently there is an irrelevant length scale, similar to the one we had above. Below $p\approx0.05$ the

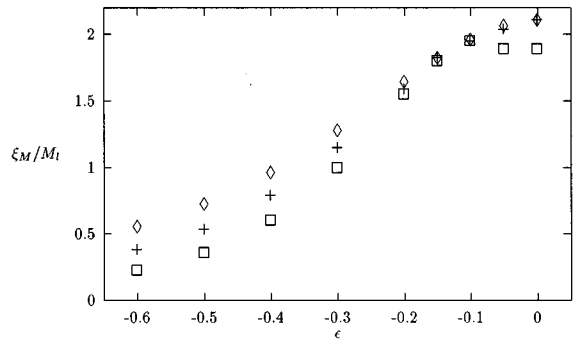

FIG. 11. Renormalized localization length ξ_M/M_l as a function of energy ϵ for a system with reduced U(2) mixing between the levels ($p=0.3$). $\diamond$'s correspond to $M=16$, $+$'s to $M=32$, and $\square$'s to $M=64$ system widths. A fit to a scaling form yields two extended states at $\epsilon=\pm0.16$, with $\nu=2.5$

TABLE I. Symmetry classes of random phases.

Group	Link phases α,β	No. of energies with extended states	ν
SO(2)	arbitrary	1	2.2
SU(2)	0	1	1.1
U(2)	random	2	2.5

behavior is close to that of the SU(2) (i.e., $p=0$) case, i.e., Figs. 9 and 10. Thus we have a U(2) to SU(2) phase transition at a finite p, $p\approx 0.2$.

We summarize our results in Table I. The table shows the different symmetries involved with their critical properties.

V. DISCUSSION

We have studied two types of systems: (i) nondegenerate states with random mixing and random scalar potential and (ii) degenerate states with randomness only in the mixing terms. The system with nondegenerate states is relevant to two types of experimentally studied cases. The first case is where nondegeneracy is represented by Landau-level splitting. We find that the lower Landau level has a minimum as a function of magnetic field, consistent with the floating scenario.[10,11] This result accounts for a transition from a Hall liquid to an insulator at both high and low fields, as observed experimentally.[12]

The second case is where nondegeneracy is represented by the Zeeman spin splitting. In this case the bare splitting Δ (which is $g^*\mu_B B/E_1$ in the simplest case) can cross the value ≈ 0.5 where level repulsion crosses into level attraction. We predict, therefore, that the spin splitting of the extended states is larger (smaller) than the bare Zeeman splitting at low (high) fields. To estimate the field corresponding to $\Delta\approx 0.5$ we use data[27] on the temperature scaling of the conductance peak in GaAs/Al_xGa_{1-x}As, which show that the low-temperature scaling of the $N=0\downarrow$ peak near $B=6$ T is modified at a crossover temperature of ≈ 0.3 K. An analysis of tunneling through saddle-point barriers[25] shows that the crossover temperature is $T_1=\hbar U/2\pi m\omega_c$, where $U(=U_x=U_y)$ is the barrier curvature. Since $T_1\ll\omega_c\approx 120$ K at $B=6$ T (using an effective mass[28] of $m/m_0\approx 0.07$) Eq. (4) yields $E_1\approx\hbar U/m\omega_c=2\pi T_1\approx 2$ K and $(\hbar U/m)^{1/2}\approx 15$ K. Using the bulk value[20] $g^*=0.44$, we obtain $\Delta\approx 1$, i.e., level attraction is predicted above $B\approx 4$ T (where $\Delta\approx 0.5$).

Spin splitting of extended states can be directly probed by ESR; the extended electromagnetic wave couples dominantly the extended states. Experimental data[20] on Landau levels $N=0,1,2$ show a spin splitting that is nonlinear in B and was fitted by a quadratic polynomial. Band-structure calculations[28,29] show that at large fields the pure system has a spin splitting of the form $\Delta E_0=g^*\mu_B B+\nu_N$, assuming[28] $\nu_N\ll\omega_c$ (in the more recent calculation[29] the linear form is valid for $N=0, B>6$ T).

The nonlinearity is best seen in the $N=0$ data, which span $B=8-14$ T and is clearly nonlinear in the range $8-12$ T. The band-structure calculations[28,29] predict linear behavior, at least at $B>6$ T. We propose then that the deviation from linearity is due to localization effects, i.e., level attraction. Note also that if indeed the ESR transition probes only extended states, it accounts for the remarkably low linewidth[20] of 50 mT.

To fit the data we choose $\Delta E_0=g^*\mu_B B+\nu_0$, with $g^*m/2m_0=0.018$ and $\nu_0=0$ (i.e., for[28] $m/m_0=0.07$ we have $g^*=0.51$). The parameter Δ of Fig. 3 is now $\Delta=\Delta E_0/E_1$, allowing the data of Fig. 3 to be replotted as the splitting $\Delta E=E_1(\epsilon_2-\epsilon_1)$ in Fig. 4. The experimental data could also be fitted with a smaller g^* by increasing ν_0, e.g., $g^*=0.44$ with $\nu_0=11$ GHz. The splitting in frequency units is given by $(U/m)^{1/2}=310$ GHz, while the field scale is set by $\omega_c(U/m)^{1/2}=1.3B$ T.

Figure 4 shows nonlinear behavior with a decreasing slope for $B>8$ T, in agreement with the experimental data.[20] Below 8 T we predict a different trend with the energy splitting crossing the bare one at ≈ 4 T (Fig. 4) and becoming larger than the bare splitting at $B<4$ T. (Recall that the bare splitting itself, which should be determined by a band-structure calculation, may be nonlinear in B for these lower fields.[28,29]) We propose then that extending the ESR data to lower and higher fields can serve as a unique tool for testing our predictions for level attraction and repulsion.

We have also studied the network model with random mixing of two degenerate states, while the scalar potential is periodic (nonrandom). The random part of the transfer matrix Eq. (12) is then an SU(2) matrix. We believe that this model corresponds to that of Hikami *et al.*[21] Eq. (13). There are, however, some differences. (a) The continuum translation symmetry of the free particle term in Eq. (13) is replaced by a periodic potential with extended states in the band of Eq. (14). This band resembles the continuum one for small α,β. (b) The random fields h_x,h_y of Eq. (12) correspond in our case to a general SU(2) matrix, i.e., we have also a random h_z component. While Eq. (13) including a random h_z was not explicitly studied, we believe that the noncommutative Pauli matrices σ_x,σ_y generate σ_z terms in the time evolution (or in perturbation theory) and the models are therefore equivalent.

Our results for the SU(2) model show that for small but finite α,β a single extended state appears at $\epsilon=0$, though the localized nature of nearby states appears only at unusually wide strips ($M=128$). This indicates that the phases α,β produce an additional (irrelevant) length scale, which renders numerical analysis more difficult. Remarkably, for the choice $\alpha=\beta=0$ the irrelevant length scale disappears and we find a clear single extended state at $\epsilon=0$. Finite-size scaling is well obeyed (Fig. 10) and an exponent $\nu=1.1$ is found. Thus the SU(2) network model forms a distinct universality class.

Our SU(2) data are inconsistent with the argument of Lee[22] and with the numerical study of Minakuchi and Hikami.[17] The argument of Wei *et al.* is qualitative and applies to slowly varying random fields $\mathbf{h}(\mathbf{r})$, while in our case $\mathbf{h}(\mathbf{r})$ is uncorrelated between unit cells. We do not expect that this will change critical properties since correlations will vanish along long loops in both cases. The numerical data of Minakuchi and Hikami, who study Eq. (13), show three extended states. At present we cannot account for this discrepancy with regard to the location of extended states; although Eq. (13) is defined differently from our SU(2) model, the two should be equivalent, as discussed above.

Experimental realizations of the SU(2) model correspond to systems with dominant spin-orbit coupling. We predict

that in a usual random system that has spin-split levels, increasing the strength of spin-orbit coupling would shift the extended states so that they approach each other, until at some critical value of the spin-orbit coupling, the energies of these two extended states would merge. We simulated this situation by allowing randomness in link phases to vary in the range $p[-\pi,\pi]$ range. We find that below $p\approx 0.2$ the system behaves like an SU(2) one, i.e., an extended state (or states) at the single energy of the band center.

ACKNOWLEDGMENTS

We wish to thank Professor J. T. Chalker for valuable discussions, for sending his data to us, and for hospitality during the visit of one of us (V. K.). We also thank M. Feingold and Y. Meir for useful discussions. V. K. also thanks Dr. B. Huckestein and Dr. D. Polyakov for valuable discussions.

APPENDIX A: TEST FOR SUBLOCALIZATION

The simplest argument for deriving the 7/3 exponent[4] is based on the semiclassical picture. An electron with energy $E\neq 0$ follows semiclassical constant potential contours[3] on clusters of size of the percolation length ξ_p, which, according to percolation theory, diverges as $\xi_p\sim|E|^{-4/3}$. An electron can propagate to a distance $r\gg\xi_p$ by tunneling events between clusters, each event reducing the wave function by a factor $\exp(-a|E|)$, where a depends on potential barrier parameters. These tunneling events occur at saddle points in the potential that are on the infinite percolating cluster at $E=0$. Assuming that these saddle points are homogeneously distributed, i.e., their number is r/ξ_p, we find that the total wave-function decay is

$$[\exp(-a|E|)]^{r/\xi_p}=\exp(-r/\xi). \tag{A1}$$

Hence the localization length $\xi\sim\xi_p/|E|\sim|E|^{-7/3}$.

We wish to test the homogeneity assumption, i.e., whether the number of tunneling events is r/ξ_p. In the theory of percolation the infinite cluster at the critical energy has a backbone consisting of alternating sequence of singly connected (''red'') bonds and multiply connected (''blue'') bonds.[30–32] It is conceivable that tunneling occurs at red bonds of the infinite cluster, i.e., bonds whose elimination disconnects the infinite cluster. Analytic[32] and numerical[33] studies show that the number of red bonds $L_{\rm red}$ between two points separated by a correlation length ξ_p diverges as E^{-1}; therefore, at the scales $r=\xi_p\sim E^{-4/3}$ we obtain $L_{BB}\sim r^{3/4}$. If we assume that the number of tunneling events is $(r/\xi_p)^{3/4}$, the derivation of the localization length Eq. (A1) is now modified to $\exp[(-aE)(r/\xi_p)^{3/4}]\sim\exp[-(r/\xi)^{3/4}]$. The consequences are that now the localization length exponent is modified $\xi\sim E^{-8/3}$ and more significantly that sublocalization appears with a weaker $\exp[-(r/\xi)^{3/4}]$ decay. To check this possibility consider how it affects finite-size scaling and in particular the region of localized states.[34] Suppose that wave function on an $M\times M$ square decreases as $\exp[-(M/\tilde{\xi}_M)^{\beta}]$. Then at distance $r>M$, where M is the width of the strip, it decays as in a 1D strip, i.e., as $\exp[-(M/\tilde{\xi}_M)^{\beta}(r/M)]=\exp[-r/\xi_M]$, and ξ_M is the value that we calculate numerically; hence $\xi_M=(\tilde{\xi}_M/M)^{\beta}M$. On on the other hand, by the scaling hypothesis $\tilde{\xi}_M/M=f(\xi/M)$, which for $\xi\ll M$ yields $\tilde{\xi}_M/M=\xi/M$ and therefore $\xi_M/M=(\xi/M)^{\beta}$. Therefore an asymptotic tangent to the fitting curve of $\log(\xi_M/M)$ versus $\log(M/\xi)$ should have a slope $-\beta$ ($-3/4$ if the idea of red bonds is valid). We perform optimization procedure using our results as well as data from Chalker and Coddington.[35] The fitting curve (Fig. 12) and its tangent in the range $\xi\ll M$ show conclusively that β cannot be distinguished from unity and therefore the localized wave functions decay exponentially.

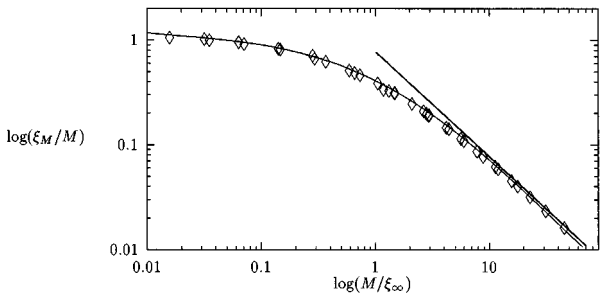

FIG. 12. Fit of the data for the one-channel model: ξ_M/M versus M/ξ and a tangential straight line with slope equal to unity.

APPENDIX B: MIXING OF LANDAU LEVELS

We wish to estimate the mixing probability of Landau levels on the links, i.e., far from saddle points. We consider then the tunneling rate between Landau levels in a weakly perturbed harmonic potential. We choose the potential on the links as $V(x,y)=(1/2)\tilde{U}(x^2+y^2)-(\tilde{U}/\lambda)y^3$; λ is a a measure of the correlation length of the potential. We perform a standard change of variables

$$\hat{\pi}=\hat{\mathbf{p}}-\frac{e\hat{\mathbf{A}}}{c},\quad \hat{X}=x-\frac{c\hat{\pi}_y}{eB},\quad \hat{Y}=y+\frac{c\hat{\pi}_x}{eB}. \tag{B1}$$

$\hat{X}$ and $\hat{Y}$ are slow guiding center coordinates and $\hat{\pi}_{x,y}$ are operators of fast cyclotron motion. A Schrödinger equation for the fast variables (choosing $c\hat{\pi}_x/eB=z$ as a coordinate and treating $\hat{X}$ and $\hat{Y}$ adiabatically) has the form

$$\left[\left(\frac{1}{2m}+\frac{\tilde{U}}{2m^2\omega_c^2}\right)\left(\frac{d}{dz}+\frac{\tilde{U}m^2\omega_c X}{m\omega_c^2+\tilde{U}}\right)^2+\frac{m}{2}\left(\omega_c^2+\frac{\tilde{U}}{m}-\frac{3\tilde{U}Y}{\lambda m}\right)\left(z-\frac{\tilde{U}Y/m-(3\tilde{U}/\lambda m)Y^2}{\omega_c^2+\tilde{U}/m-(6\tilde{U}/\lambda m)Y}\right)^2+\frac{\tilde{U}}{\lambda}z^3\right]\psi_n(z;X,Y)$$
$$=E_n(X,Y)\psi_n(z;X,Y). \tag{B2}$$

Eigenvalues of Eq. (B2) can be interpreted[36] as local nonequidistant Landau levels $E_n(X,Y)$ depending on the classical guiding center coordinates.

We estimate the tunneling rate between neighbor Landau levels using Dykhne's formula[37,38]

$$P_{n,n+1}\sim\exp\left[-(2/\hbar)\ \mathrm{Im}\int_0^{t_c}(E_{n+1}-E_n)dt\right], \quad \text{(B3)}$$

where $E_{n+1}>E_n$ for all real times and t_c is a point in the complex time plane where they cross. We solve Eq. (B2) keeping X and Y as fixed parameters and obtain to first order in $1/\lambda$

$$E_{n+1}-E_n\approx\hbar\omega_c\left(1+\frac{\widetilde{U}}{m\omega_c^2}-\frac{3\widetilde{U}Y/\lambda}{m\omega_c^2+\widetilde{U}}\right). \quad \text{(B4)}$$

Note that we are considering quasibound states near the local minimum of $V(x,y)$, i.e., $Y\ll\lambda$. We solve equations of motion for Y in a harmonic potential, substitute this solution into Eq. (B4), and find

$$t_c=\frac{\pi}{2}\frac{m\omega_c}{\widetilde{U}}\pm i\frac{m\omega_c}{\widetilde{U}}\ln\frac{2\lambda(m\omega_c^2+\widetilde{U})^2}{3m\widetilde{U}\omega_c^2A}, \quad \text{(B5)}$$

where A is the amplitude of oscillations in the Y direction. Note that $\widetilde{U}A$ is a measure of the center coordinate energy, which corresponds to the width of a Landau band; since this width is less than or on the order of $\hbar\omega_c$ we have $A\lesssim\sqrt{\hbar\omega_c/\widetilde{U}}=l\sqrt{m\omega_c^2/\widetilde{U}}$, where l is the cyclotron length. We find crossings at conjugate points, as one expects for real Hamiltonians.[38] Evaluating, then, Eq. (B3), we find that the main contribution to the tunneling (in this adiabatic approximation) is independent on n and proportional to

$$P_{n,n+1}\sim\exp\left(-\frac{m\omega_c^2+\widetilde{U}}{\widetilde{U}}\ln\frac{2\lambda(m\omega_c^2+\widetilde{U})^2}{3l\sqrt{m\widetilde{U}\omega_c^3}}\right). \quad \text{(B6)}$$

For transitions from n to $n+\Delta n$ the term in the exponent is multiplied by Δn.

*Present address: Max-Planck-Institut für Kernphysik, Postfach 10 39 80, D-69029, Heidelberg, Germany.

[1] *The Quantum Hall Effect*, edited by R. E. Prange and S. M. Girvin (Springer-Verlag, Berlin, 1985).

[2] A. M. M. Pruisken, Phys. Rev. Lett. **61**, 1297 (1988).

[3] S. A. Trugman, Phys. Rev. B **27**, 7539 (1983).

[4] G. V. Milnikov and I. M. Sokolov, Pis'ma Zh. Éksp. Teor. Fiz. **48**, 494 (1988) [JETP Lett. **48**, 536 (1988)].

[5] T. Ando, J. Phys. Soc. Jpn. **53**, 3126 (1984).

[6] J. T. Chalker and P. D. Coddington, J. Phys. C **21**, 2665 (1988).

[7] S. Koch, R. J. Haug, K. v. Klitzing, and K. Ploog, Phys. Rev. B **46**, 1596 (1992).

[8] E. Abrahams, P. W. Anderson, D. C. Licciardello, and T. V. Ramakrishnan, Phys. Rev. Lett. **42**, 673 (1979).

[9] P. A. Lee and D. S. Fisher, Phys. Rev. Lett. **47**, 882 (1981); A. MacKinnon and B. Kramer, *ibid.* **47**, 1546 (1981); in *The Application of High Magnetic Fields in Semiconductor Physics*, edited by G. Landwehr, Lecture Notes in Physics Vol. 177 (Springer, Berlin, 1983), p. 74.

[10] D. E. Khmelnitskii, Phys. Lett. **106**, 182 (1984); Pis'ma Zh. Éksp. Teor. Fiz. **38**, 454 (1983) [JETP Lett. **38**, 556 (1983)].

[11] R. B. Laughlin, Phys. Rev. Lett. **52**, 2304 (1984).

[12] H. W. Jiang, C. E. Johnson, K. L. Wang, and S. T. Hannahs, Phys. Rev. Lett. **71**, 1439 (1993); T. Wang, K. P. Clark, G. F. Spencer, A. M. Mack, and W. P. Kirk, *ibid.* **72**, 709 (1994); R. J. F. Hughes, J. T. Nicholls, J. E. F. Frost, E. H. Linfield, M. Pepper, C. J. B. Ford, D. A. Ritchie, G. A. C. Jones, E. Kogan, and M. Kaveh, J. Phys. Condens. Matter **6**, 4763 (1994); A. A. Shashkin, G. V. Kravchenko, and V. T. Dolgopolov, Pis'ma Zh. Éksp. Teor. Fiz. **52**, 215 (1993) [JETP Lett. **58**, 220 (1993)]; I. Glozman, C. E. Johnson, and H. W. Jiang, Phys. Rev. Lett. **74**, 594 (1995).

[13] D. K. K. Lee and J. T. Chalker, Phys. Rev. Lett. **72**, 1510 (1994).

[14] D. K. K. Lee, J. T. Chalker, and D. Y. K. Ko, Phys. Rev. B **50**, 5272 (1994).

[15] Z. Wang, D. H. Lee, and X. G. Wen, Phys. Rev. Lett. **72**, 2454 (1994).

[16] C. B. Hanna, D. P. Arovas, K. Mullen, and S. M. Girvin, Phys. Rev. B **52**, 5221 (1995).

[17] K. Minakuchi and S. Hikami, Phys. Rev. B **53**, 10 898 (1996).

[18] V. Kagalovsky, B. Horovitz, and Y. Avishai, Phys. Rev. B **52**, 17 044 (1995).

[19] T. V. Shahbazyan and M. E. Raikh, Phys. Rev. Lett. **75**, 304 (1995).

[20] M. Dobers, K. v. Klitzing, and G. Weimann, Phys. Rev. B **38**, 5453 (1988).

[21] S. Hikami, M. Shirai, and F. Wegner, Nucl. Phys. B **408**, 415 (1993).

[22] D. K. K. Lee, Phys. Rev. B **50**, 7743 (1994).

[23] H. A. Fertig and B. I. Halperin, Phys. Rev. B **36**, 7969 (1987).

[24] B. Huckestein and B. Kramer, Phys. Rev. Lett. **64**, 1437 (1990).

[25] V. Kagalovsky, B. Horovitz, and Y. Avishai, Europhys. Lett. **31**, 425 (1995).

[26] S. N. Evangelou, Phys. Rev. Lett. **75**, 2550 (1995).

[27] H. P. Wei, S. Y. Lin, D. C. Tsui, and A. M. M. Pruisken, Phys. Rev. B **45**, 3926 (1992).

[28] R. Lassnig, Phys. Rev. B **31**, 8076 (1985).

[29] G. Lommer, F. Malcher, and U. Rössler, Superlatt. Microstruct. **2**, 273 (1986).

[30] H. E. Stanley, J. Phys. A **10**, L211 (1977).

[31] R. Pike and H. E. Stanley, J. Phys. A **14**, L169 (1981).

[32] A. Coniglio, J. Phys. A **15**, 3829 (1982).

[33] D. C. Hong and H. E. Stanley, J. Phys. A **16**, L475 (1983).

[34] C. J. Lambert and G. D. Hughes, Phys. Rev. Lett. **66**, 1074 (1991).

[35] J. T. Chalker (private communication).

[36] A. Entelis and S. Levit, Phys. Rev. Lett. **69**, 3001 (1992).

[37] A. M. Dykhne, Zh. Éksp. Teor. Fiz. **41**, 1324 (1961) [Sov. Phys. JETP **14**, 941 (1962)].

[38] J. Moody, A. Shapere, and F. Wilczek, in *Geometric Phases in Physics*, edited by A. Shapere and F. Wilczek (World Scientific, Singapore, 1989), p. 160.